Thermal Science and Engineering (2022) Volume 5 Issue 2
doi:10.24294/tse.v5i2.1533

ORIGINAL RESEARCH ARTICLE

Energy saving analysis of photovoltaic roof based on MATLAB

Hui Luo*, Kequn Li

School of energy and power engineering, Shanghai University of Technology, Shanghai 200093, China. E-mail: Charlottebrisk@163.com

ABSTRACT

One-dimensional unsteady theoretical models of three different photovoltaic module installation modes are established. Through MATLAB modeling and simulation, the influence of photovoltaic modules on roof heat transfer in different layout modes is compared. Comparing with ordinary roof, the shading effect of photovoltaic roof in summer and heat preservation effect in winter was analyzed. The results show that the PV roof layout with ventilation channel is better in summer. The proof layout with closed flow channel is better in winter.

Keywords: Photovoltaic Roof; MATLAB; Heat Transfer Model; Thermal Energy

ARTICLE INFO

Received: 5 June 2022
Accepted: 8 July 2022
Available online: 20 July 2022

1. Introduction

The integration of solar energy building is to combine solar energy products with buildings and integrate solar energy system with building characteristics, so as to achieve the organic combination of solar energy and buildings[1]. Photovoltaic architecture integration is an embodiment of solar architecture integration, which uses photovoltaic cells to replace part of building materials and provide electric energy for buildings. Photovoltaic cells have replaced part of the building materials, thus have changed the thermal performance of photovoltaic modules.

The electrical properties of photovoltaic modules have been studied extensively. Brinkworth *et al.*[2] studied the interaction between the electrical performance of photovoltaic modules and building load, and focused on the electrical performance of photovoltaic modules; Yang *et al.*[3] studied the heat transfer performance and electrical performance of photovoltaic roofs with ventilation channels; Ji *et al.*[4] conducted annual numerical simulation of electrical energy and heat gain of photovoltaic walls facing east, south and west with or without natural ventilation; Yutaka *et al.*[5] studied the influence of large-scale use of photovoltaic system on building cooling load. The above literature adopts steady-state model and simple electrical performance model for photovoltaic modules, but the influence of photovoltaic modules on building cold and heat load and different photovoltaic integration methods are not considered in the analysis. Ren *et al.*[6] discussed the tion between rooftop PV and building load and established an unsteady model, but it was not applied to fields other than housing construction.

In this paper, photovoltaic architecture is applied to the solar assisting passenger car roof, and one-dimensional unsteady models of three different photovoltaic module installation modes are established.

The influence of different PV installation types on roof thermal load was compared, and the shading effect of PV roof in summer and insulation effect in winter were analyzed.

A common roof was set as the control group, and the other three photovoltaic panels were arranged on the roof with different installation methods, as shown in **Figure 1**.

2. Theoretical model

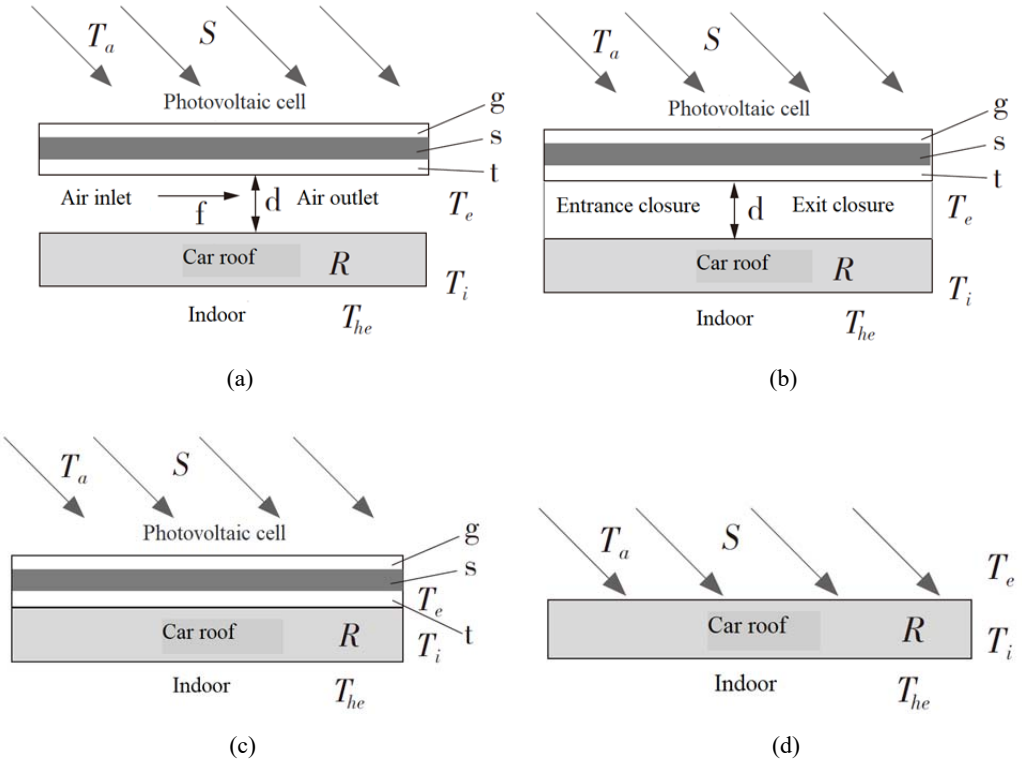

Figure 1. Schematic diagram of photovoltaic roof structure with different arrangement modes. **(a)** Photovoltaic roof with ventilation channels; **(b)** photovoltaic roof with closed ventilation channels; **(c)** attached PV roof; **(d)** ordinary car roof.

2.1 Photovoltaic roof model of ventilation channel

The whole model is mainly based on the heat transfer model of the photovoltaic roof, and the calculation of the cooling and heat load of the roof is mainly carried out by steady-state method, and the calculation is carried out by solving the temperature of the model.

Figure 2 shows the photovoltaic roof heat transfer network with ventilation channels. The characters g, s, t respectively refers to the upper glass cover plate, photovoltaic cell and lower backplane of the photovoltaic panel module; the letter f refers to the air in the ventilation passage; T_a, T_f, T_e, T_i, T_{he} are respectively: ambient temperature, air temperature in the air passage, temperature on the outer surface of the roof, and inside roof surface temperature and the temperature inside the car. R is the thermal resistance of the layer. Subscripts c, r, and d refer to convection, radiation, and heat conduction respectively. As other arrangement of the heat transfer network is not complex, so they are not displayed.

2.1.1 Heat transfer model of photovoltaic roof

(1) Heat transfer of photovoltaic modules

The photovoltaic module is divided into three layers, namely, the upper glass cover panel, photovoltaic cell and lower backplane. The upper cover plate is generally made of tempered glass with a very high light transmittance of 0.9. Energy balance equation of upper cover plate[7,8]:

$$m_g C_g \frac{dT_g}{dt} = S\alpha_g A(1-\rho_{o,g}) + h_w A(T_a - T_g) + h_{gs} A(T_s - T_g) + q_{r,ga} \quad (1)$$

Where: m_g—mass of upper glass, kg; C_g—specific heat capacity of the upper glass,

J/(kg·K); S—solar radiation intensity, W/m^2; α_g—absorption rate of upper glass; A—area of upper glass, m^2; $\rho_{o,g}$—reflectivity of the upper glass; h_w—convective heat transfer coefficient, W/(m^2·K); h_{gs}—Heat transfer coefficient between battery and glass, W/(m^2·K); $q_{r,ga}$—the heat transfer between the glass and the environment, W.

The heat transfer coefficient of photovoltaic cell and the upper glass is calculated with Equation (2):

$$h_{gs} = 1 \Big/ \left(\frac{d_g/2}{k_g} + \frac{d_s/2}{k_s} \right) \tag{2}$$

Where: d_g—thickness of the upper glass, m; d_S—photovoltaic (PV) thickness of the battery, m; k_g—thermal conductivity of the upper glass, W/(m·K); k_s—thermal conductivity of photovoltaic cell, W/(m·K).

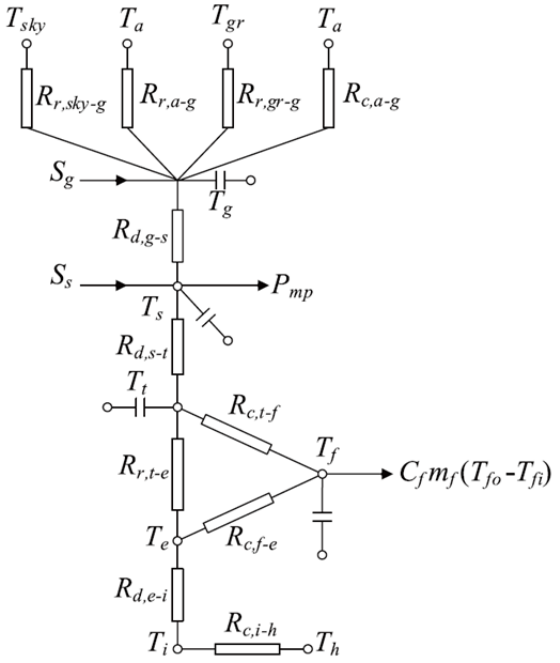

Figure 2. Heat transfer network of photovoltaic roof with ventilation channels**.**

After solar cells receive solar radiation, part of the energy transfer into electricity, and part of the energy transfer into heat energy, in the form of heat conduction to other media. The energy balance equation of photovoltaic cells is shown in Equation (3):

$$m_s C_s \frac{dT_s}{dt} = S\alpha_s A(1-\rho_{o,g})(1-\alpha_g) + h_{st}A(T_t - T_s) + h_{gs}A(T_g - T_s) - P_{mp} \tag{3}$$

Where: m_s—mass of photovoltaic cells, kg; C_S—specific heat capacity of the upper glass cover plate, J/(kg·K); α_S—absorption rate of photovoltaic cells; h_{st}—Heat transfer coefficient between photovoltaic cell and lower backplane, W/(m^2·K); P_{mp}—the output power of the photovoltaic cell, W.

In the equilibrium equation shown in Equation (3), h_{st} refers to the heat transfer coefficient between photovoltaic cell and lower backplane, as Equation (4) shows:

$$h_{st} = 1 \Big/ \left(\frac{d_t/2}{k_t} + \frac{d_s/2}{k_s} \right) \tag{4}$$

The meanings of the items in Equation (4) are the same as those in Equation (2).

The subscript t refers to the lower backplane and subscript s refers to the photovoltaic cell.

Energy balance equation for the lower backplane:

$$m_t C_t \frac{dT_t}{dt} = h_{st}A(T_s - T_t) + h_{tf}A(T_f - T_t) + A\delta(T_e^4 - T_t^4) \Big/ \left(\frac{1}{\varepsilon_t} + \frac{1}{\varepsilon_e} - 1 \right) \tag{5}$$

In the energy balance equation shown in Equation (5), the subscript e refers to the outer surface of the car roof.

The convective heat transfer coefficient of the air in the ventilation duct is calculated with Equation (6)[9]:

$$h_{tf} = \frac{Nuk_f}{D_f} = \left(5.801 + \frac{0.086 Re D_h}{L} \right) k_f / D_h \tag{6}$$

Where: Nu—Nusselt number; k_f—thermal conductivity of air, W/(m·K); D_h—hydraulic diameter, m; Re—Reynolds number; L—length of ventilation duct, m.

(2) Air heat transfer in the ventilation passage

Conduct balance analysis of air energy in the passage, and Equation (7) is obtained[9-11]:

$$m_f C_f \frac{dT_f}{dt} = h_{fe}A(T_e - T_f) + h_{tf}A(T_t - T_f) - m_{fr}C_f(T_{fo} - T_{fi}) \tag{7}$$

Where: hfe—convective heat transfer coefficient of the air on the outer surface of the roof and in the channel, W/(m^2·K); h_{tf}—Convective heat transfer coefficient of air in lower backplane and

channel, W/(m^2·K); m_{fi}—the mass flow rate of air in the passage, kg/s; T_{fo}—air temperature at the outlet of the flow passage, K; T_{fi}—air temperature at the inlet of the channel, K.

(3) Heat transfer of the car roof

According to the heat transfer analysis of the roof, the one-dimensional unsteady heat transfer equation of the roof can be obtained:

$$\frac{\partial T}{\partial t} = \alpha_d \frac{\partial^2 T}{\partial x^2} \tag{8}$$

Where: α_d—thermal diffusivity of roof materials, $\alpha_d = \frac{\lambda_e}{\partial x^2}$, m^2/s.

The roof is divided into four layers, each made of a different material. Each layer has a different thermal diffusivity α_d.

Based on the energy balance equation of the roof, the boundary conditions are written:

$$-\lambda_e \frac{\partial T}{\partial x}\bigg|_{x=0} = h_{fe}(T_e - T_f) + \delta(T_e^4 - T_t^4) \Big/ \left(\frac{1}{\varepsilon_t} + \frac{1}{\varepsilon_e} - 1\right) \tag{9}$$

$$-\lambda_i \frac{\partial T}{\partial x}\bigg|_{x=d_d} = h_{ih}(T_i - T_{he}) \tag{10}$$

Where, it is assumed that the interior air temperature in winter is 16 °C. In summer, the air temperature inside the car is 28 °C. There are heat exchange between the interior air and the interior surface of the roof, I which h_{ih} is 29W/(m^2·K).

2.1.2 Electrical performance model of photovoltaic modules

The output power of photovoltaic cells selected in this paper is 340 W under standard conditions. The relationship between output power and radiation intensity and battery temperature can generally be calculated with empirical formula:

$$P_{mp} = \frac{S \cdot [\alpha + \beta \cdot (T_s - 273.15)]}{S_f \cdot A_g} \tag{11}$$

Where: α—experimental calibration constant, 550; β—the temperature coefficient of photovoltaic cells, -0.221, W/K; S_f—solar radiation intensity under standard conditions, 1,000 W/m^2; A_g—photovoltaic cell area, m^2; T_s—junction temperature of photovoltaic cell, K.

2.2 Closed flow channel PV roof model

The calculation of the model with ventilated flow passage is similar to that of the model with closed flow passage. The difference lies in that model with closed flow passage has both ends of the flow passage in closed state. See **Figure 1(b)** for the physical model. The calculation equations of the two models are basically the same, but with some changes. Equation (7) is modified, because the model is closed at both ends, the third term on the right of the formula is eliminated, that is, the heat exchange caused by the air flowing in the flow channel. And the Nusselt number in Equation (6) is calculated with Equation (12)[12]:

$$Nu = 1 + 1.44\left[1 - \frac{1\ 708}{Re\cos\theta}\right]\left\{1 - \frac{1\ 708(\sin 1.8\theta)^{1.6}}{Re\cos\theta}\right\} + \left[\left(\frac{Re\cos\theta}{5\ 830}\right)^{1/3} - 1\right] \tag{12}$$

Where: θ—tilt angle of photovoltaic panel group, °.

In Equation (12), square brackets mean that when the value of this item is less than 0, it is calculated as 0. The rest formulas in the model are the same as those in the model with ventilation channels.

2.3 Attach and install PV roof model

Photovoltaic panels are attached to the roof model, as shown in **Figure 1(c)**. In Equation (5), the second and third terms on the right are replaced by the thermal conductivity equation between the photovoltaic panel and the outermost material of the roof. Therefore, the external conditions of the roof become the thermal conductivity equation between different solids[13]. The calculation formula is as follows:

$$m_t C_t \frac{dT_t}{dt} = h_{st}A(T_s - T_t) + h_{st}A(T_f - T_t) \tag{13}$$

$$-\lambda_e \frac{\partial T}{\partial x}\bigg|_{x=0} = h_{st}(T_t - T_s) \tag{14}$$

The inner surface boundary conditions of the roof attached to the installation model are the same as those of the photovoltaic roof model with airflow passage, as shown in Equation (9).

2.4 Ordinary roof model

The ordinary roof model does not include

photovoltaic panels and ventilation channels, as in **Figure 1(d)**. The heat transfer model of the vehicle item is composed of Equations (8) to (10), and the boundary condition Equation (9) needs to be modified. The modified calculation formula is shown in Equation (15):

$$-\lambda_e \frac{\partial T}{\partial x}\bigg|_{x=0} = S\alpha_e + h_w(T_e - T_f) + q_{r,ea}/A \tag{15}$$

3. Model solution

The theoretical model was programmed by MATLAB, and ode15 s variable step size algorithm was used to solve *s*. The thermal physical parameters of PV module and roof structure are shown in **Table 1**.

Other parameters of roof and PV module: glass cover absorption rate is 0.06; reflectivity of glass cover plate is 0.04; emissivity of glass cover plate is 0.9; absorption rate of photovoltaic cell is 0.893; emissivity of roof is 0.9; optically inclined angle is 0°; model length is 1.6 m, model width is 1 m; ventilation channel spacing is 0.2 m.

Table 1. Thermophysical parameters of car roof and PV modules

Parts	Materials	Heat conductivity coefficient/(W/(m·K))	Density/(kg/m^3)	Specific heat capacity/(J/(kg·K))	Thickness/mm
Photovoltaic module	Glass cover-plate	1.04	2,500	835	4.0
	Photovoltaic cell	150.00	1,650	700	0.3
	Backplane	0.14	1,475	1,130	5.0
Roof material	Steel plate	48.15	7,850	481	8
	Air interlayer	0.0251	1.205	1,005	20
	PU polyurethane	0.0230	33	1,380	30
	PVC board	0.1400	1,400	2,510	3

4. Heat transfer simulation analysis of photovoltaic roof model

4.1 Heat transfer analysis of photovoltaic roof in summer

During the calculation and simulation of photovoltaic roof heat transfer under sunny day type in summer, the indoor temperature was set at 28 ℃ according to the environmental parameters of sunny day type. The impact of different layout on the roof heat was analyzed. The solar radiation intensity and temperature under the sunny day pattern are shown in **Figure 3**.

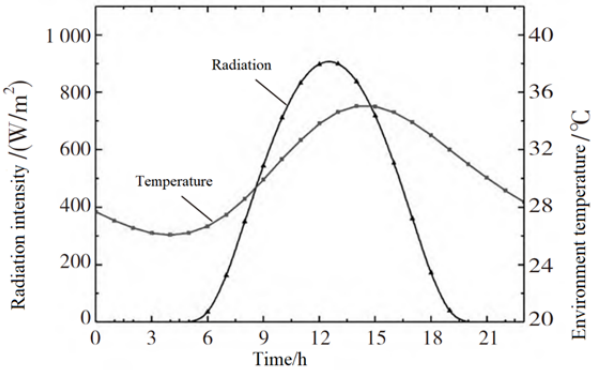

Figure 3. Hourly radiation and temperature of sunny days in summer**.**

Three kinds of light with different arrangement are obtained through simulation calculation of temperature distribution on the inner surface of volt roof and ordinary roof.

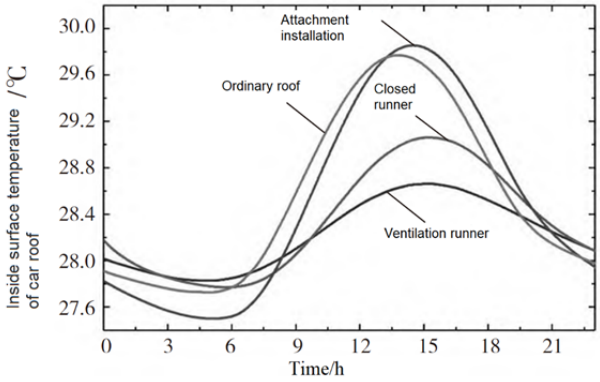

Figure 4. Temperature of car roof interior surface in different arrangements**.**

As shown in **Figure 4**, the inner surface temperature of the roof of the four groups of roof models all changed with the change of ambient temperature and radiation intensity. But their temperature peaks are markedly different. It can be seen from the figure that the peak temperature of the inner surface of the roof with ventilation passage is only 28.6 ℃; the peak temperature of the inner surface of the roof with closed runner is 29 ℃. The peak temperature of the inner surface of the roof with photovoltaic panels attached and installed and the

ordinary roof was the highest, which was 29.8 ℃ and 29.7 ℃ respectively, showing little difference between the two.

The interior surface temperature of the roof with ventilation ducts is the lowest. Although photovoltaic panels absorb a lot of radiant energy, the heat generated in the process of photoelectric conversion is taken away by the forced convection caused by bus driving, and the heat passed into the car through the air passage is reduced a lot.

Based on the temperature of the inner surface of the roof and the design temperature of the interior of the car, the roof heat and the roof cooling load at 8–21 during the air conditioning opening stage of the bus can be calculated, as shown in **Figure 5** and **Figure 6**.

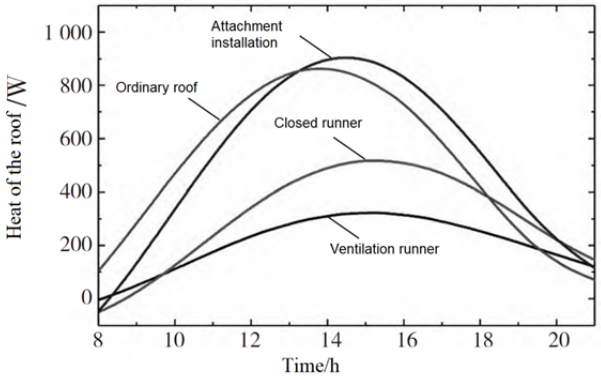

Figure 5. Heat gain of car roof in different arrangements.

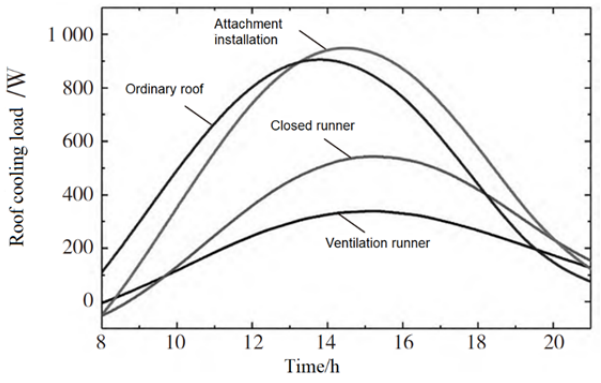

Figure 6. Cooling load of car roof in different arrangements.

In **Figure 5**, the heat of the roof is gotten with steady-state method, by calculating the temperature difference between the inner surface and the indoor design temperature. In **Figure 6**, the roof cooling load is the result obtained after a certain amount of heat is corrected. Therefore, in the diagram of temperature, heat gain and refrigeration load, the three show a consistent trend of change, and only different in the value. Peak heat gain of car roof in 4 models is: 323 W of roof with flow channel, 524 W with closed flow channel, 906 W with attached, and 866 W with regular roof.

Peak roof cooling load is: 339 W of roof with flow channel, 550 W with closed flow channel, 951 W with attached, and 909 W with ordinary roof.

Through the above analysis, it can be found that photovoltaic roof layout with ventilation channels can significantly reduce the heat gain of the roof. Compared with ordinary roof, PV roof with flow channel can reduce roof heat by 62.7%. In summer, when photovoltaic panels are arranged on the roof of buses, the photovoltaic roof arrangement scheme with ventilation channels can reduce the heat gain of the roof, and play the effect of shading and energy saving to a certain extent.

4.2 Heat transfer analysis of photovoltaic roof in winter

In winter, the temperature is low, the solar radiation intensity is weak, and the thermal insulation performance of the bus enclosure structure is insufficient, leading to the heat dissipation in the bus. In the analysis of different layout schemes in winter, the design day type was set as sunny, and the thermal insulation effect of PV panel modules on the roof under different layout methods was analyzed. The interior design temperature is 16 ℃, and daily hourly temperature and radiation are calculated as shown in **Figure 7**.

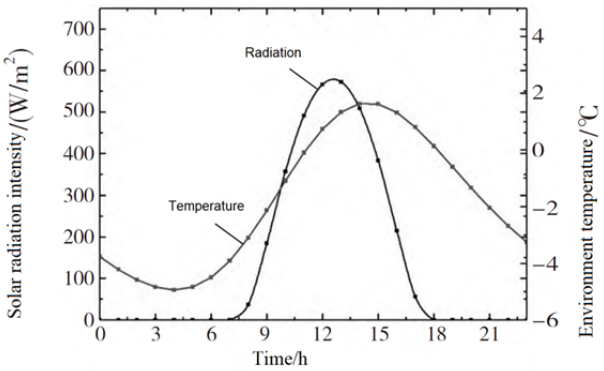

Figure 7. Design of daily hourly temperature and solar radiation in winter.

Through simulation, the temperature distribution of inner roof surface of winter passenger cars throughout the day under different arrangement modes are obtained, as shown in **Figure 8**. It can be

found that the change of inner surface temperature has the same trend with solar radiation intensity and ambient temperature of the 4 models.

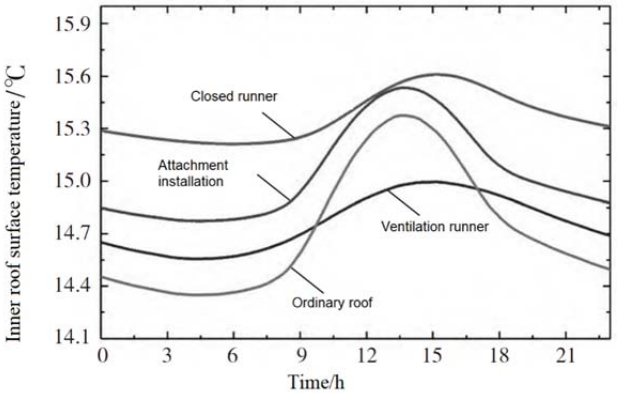

Figure 8. Hourly temperature of car roof interior surface.

Through the four models in the figure, the variation trend of roof inner surface temperature of the four models has been found. The closer the interior surface temperature of the roof with closed flow channel is to the interior design temperature, the better the thermal insulation effect. This is because the photovoltaic panel and the roof of the car formed a closed air separation layer, which reduced the loss of indoor heat to outdoor, forming a temperature box effect in the roof.

The peak highest temperatures of the inner surface of the four roof models from high to low are closed runner 15.61 ℃, attached installation 15.52 ℃, ordinary roof 15.31 ℃, and ventilation runner 14.99 ℃ in turn. The peak lowest temperatures hit around 5 p.m., which ranked from high to low are in turn closed runner 15.21 ℃, attached installation 14.77 ℃, ventilation runner 14.55 ℃, ordinary roof 14.35 ℃. The temperature of ordinary roof fluctuates the most throughout the day. At the noon when solar radiation intensified and environment temperature rises, the inner surface temperature of the ordinary roof is higher than the photovoltaic roof with ventilation runner. The main reason is that the outer surface of an ordinary car roof is exposed to intense solar radiation, which improved exterior surface temperature, reduced heat dissipation through the roof, so its inner surface temperature is higher than the PV roof with runner.

With the temperature of the interior surface of the vehicle, the heat consumption and heating load of the roof under different arrangements at 8–21 during the operation of the bus air conditioning can be calculated, as shown in **Figures 9** and **10**.

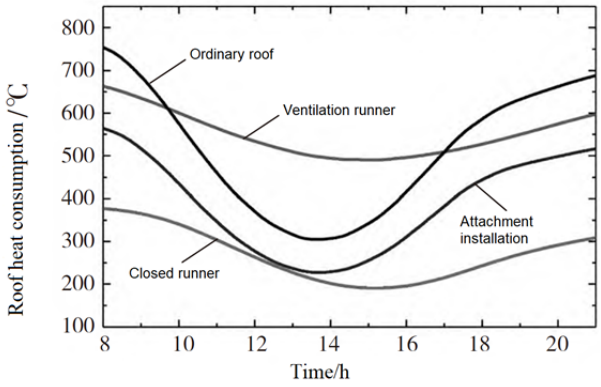

Figure 9. Heat consumption of car roof in different arrangements.

Figure 9 shows that solar radiation intensity and temperature rise high at noon time. At this time, the heat loss of the four methods is reduced, and the heat consumption of the attached roof and the ordinary roof is the most obvious. In the four models, the maximum roof heat consumption peaks are in turn closed runner 376.7 W, attached runner 566.3 W, runner 663.1 W, ordinary roof 754.3 W. The minimum roof heat consumption peaks are in turn closed runner 190.6 W, attached runner 227.2 W, ordinary roof 304.9 W, runner 490.2 W. The peak heating loads of the roof are respectively closed runner 395.6 W, attached runner 594.6 W, runner 696.3 W, ordinary roof 792.0 W. The peak minimum roof heating loads are 200.1 W for closed runner, 238.5 W for attached runner, 320.2 W for ordinary roof and 514.7 W for roof with runner respectively.

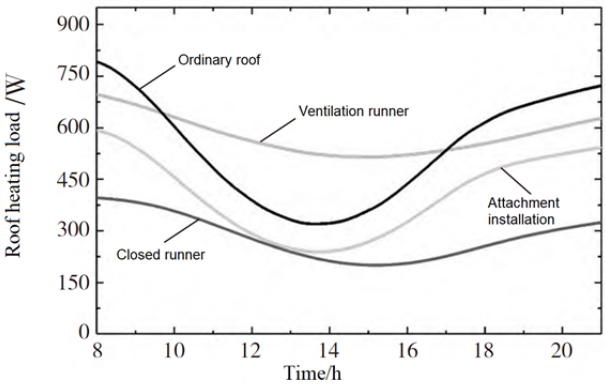

Figure 10. Heat load of car roof in different arrangements.

According to the above analysis, it can be found that the PV roof layout with closed runner in

winter can significantly reduce the heat consumption of the roof. Compared with ordinary roofs, photovoltaic roofs with closed runways consume up to 51% and at least 36.5% less heat during air conditioning operation. The photovoltaic roof layout scheme with closed runner in winter can reduce the heat consumption of the roof and to a certain extent play the effect of heat preservation and energy saving.

5. Conclusion

In this paper, four models are programmed and solved with MATLAB software. The temperature of the inner surface of the car roof is obtained through simulation calculation, and the heat transfer through the car roof under different arrangement modes is calculated. The results show that the photovoltaic panel assembly with ventilation runner can reduce the heat gain of the roof in summer. Compared with the ordinary roof, the layout with flow path can reduce the roof heat up to 62.7%. In winter, the inlet of the flow channel will be closed to form insulation on the roof, which can effectively reduce the heat consumption of the roof. Compared with ordinary roof, during the operation of air conditioning, the roof with runner can reduce at most 51%, at least 36.5% of roof heat consumption.

Conflict of interest

The authors declared that they have no conflict of interest.

References

1. Li Z. Guanyu taiyangneng guangfu faduan jishu yu jianzhu shigong de yitihua sheji yanjiu (Chinese) [Research on integrated design of solar photovoltaic power generation technology and building construction]. Low Carbon World 2020; 10(11): 84–86.
2. Brinkworth BJ, Cross BM, Marshall RH, *et al*. Thermal regulation of photovoltaic cladding. Solar Energy 1997; 61(3): 169–178.
3. Yang H, Zhu Z, Burnett J, *et al*. A simulation study on the energy performance of photovoltaic roofs. ASHRAE Transactions 2001; 107(2): 129–135.
4. Ji J, He W, Lam HN. The annual analysis of the power output and heat gain of a PV-wall with different integration mode in Hong Kong. Solar Energy Materials and Solar Cells 2002; 71(4): 435–448.
5. Yutaka G, Masako I, Yukitaka O, *et al*. Impacts of largescale photovoltaic panel installation on the heat island effect in Tokyo. Poland (Lodz): Fifth International Conference on Urban Climate. 2003. p. 181–184.
6. Ren J, LI Z, Wang Y, *et al*. Interaction between solar PV roofs and loads of the building. Acta Energiae Solaris Sinica 2008; 29(7): 849–855.
7. McClellan TM, Pedersen CO. Investigation of outside heat balance models for use in a heat balance cooling load calculation procedure. ASHRAE Transactions 1997; 103(2): 469–484.
8. Duffie JA, Beckman WA. Solar engineering of thermal processes. Hoboken: Wiley-Interscience; 2006.
9. Brinkworth BJ, Marshall RH, Ibarahim Z. A validated model of naturally ventilated PV cladding. Solar Energy 2000; 69(1): 67–81.
10. Lee WM, Infield DG, Gottschalg R. Thermal modelling of building integrated PV systems. REMIC 2001; Belfast. 2001.
11. Afonso C, Oliveira A. Solar chimneys: Simulation and experiment. Energy & Buildings 2000; 32(1): 71–79.
12. Hollands KGT, Unny TE, Raithby GD, *et al*. Free convective heat transfer across inclined air layers. Trans of ASME Journal of Heat Transfer 1976; 98(2): 189–193.
13. Yu C. Rechuandao jiqi shuzhi fenxi (Chinese) [Heat conduction and numerical analysis]. Beijing: Tsinghua University Press; 1981.
14. Shampine LF, Reichelt MW. The MATLAB ODE suite. Siam Journal on Scientific Computing 1997; 18(1): 1–22.
15. Magrab EB, Azarm S, Balachandran B, *et al*. An Engineers Guide to MATLAB. In: Gao H, Li X, Hu Z (translators). Beijing: Publishing House of Electronics Industry; 2002.